RESEARCH ARTICLE

Key Points:
- Age tracers can estimate infiltration rates in subtropical aquifers
- Tracers in riparian groundwater have a high dispersion
- Leakage from the underlying Great Artesian Basin may be significant

River infiltration to a subtropical alluvial aquifer inferred using multiple environmental tracers

S. Lamontagne[1,2], A. R. Taylor[1], J. Batlle-Aguilar[2,3], A. Suckow[1], P. G. Cook[1,2], S. D. Smith[1], U. Morgenstern[4], and M. K. Stewart[4]

[1]CSIRO Land and Water Flagship, Glen Osmond, South Australia, Australia, [2]National Centre for Groundwater Research and Training, Flinders University, Adelaide, South Australia, Australia, [3]Now at Kansas Geological Survey, University of Kansas, Lawrence, Kansas, USA, [4]GNS Science, Lower Hutt, New Zealand

Abstract Chloride (Cl$^-$), stable isotope ratios of water (δ^{18}O and δ^2H), sulfur hexafluoride (SF$_6$), tritium (^{3}H), carbon-14 (^{14}C), noble gases (^{4}He, Ne, and Ar), and hydrometry were used to characterize groundwater-surface water interactions, in particular infiltration rates, for the Lower Namoi River (New South Wales, Australia). The study period (four sampling campaigns between November 2009 and November 2011) represented the end of a decade-long drought followed by several high-flow events. The hydrometry showed that the river was generally losing to the alluvium, except when storm-derived floodwaves in the river channel generated bank recharge—discharge cycles. Using ^{3}H/^{14}C-derived estimates of groundwater mean residence time along the transect, infiltration rates ranged from 0.6 to 5 m yr^{-1}. However, when using the peak transition age (a more realistic estimate of travel time in highly dispersive environments), the range in infiltration rate was larger (4–270 m yr^{-1}). Both river water (highest δ^2H, δ^{18}O, SF$_6$, ^{3}H, and ^{14}C) and an older groundwater source (lowest δ^2H, δ^{18}O, SF$_6$, ^{3}H, ^{14}C, and highest ^{4}He) were found in the riparian zone. This old groundwater end-member may represent leakage from an underlying confined aquifer (Great Artesian Basin). Environmental tracers may be used to estimate infiltration rates in this riparian environment but the presence of multiple sources of water and a high dispersion induced by frequent variations in the water table complicates their interpretation.

1. Introduction

In many environments, exchanges between rivers and alluvial aquifers are a significant component of the water balance [*Sophocleous et al.*, 1988; *Vázquez-Suñé et al.*, 2007]. However, the exchange processes and associated fluxes are not always known because of sparse surface water and groundwater gauging [*Parsons et al.*, 2008], uncertainties in flow gauging measurements [*Schmadel et al.*, 2010], and uncertainties about the nature of the connectivity with the alluvial aquifers [*Brunner et al.*, 2009]. Yet a correct conceptual representation of groundwater-surface water interactions is required to provide greater certainty about the accuracy of the groundwater models used to manage the resource [*Brunner et al.*, 2010; *Rassam et al.*, 2013].

Sampling for environmental tracers is one strategy available to independently evaluate hydrogeological conceptual models [*Cook and Böhlke*, 2000]. Chloride concentration and the stable isotope ratios of the water molecule (δ^2H and δ^{18}O) are useful tracers for the source of groundwater in an alluvial aquifer, especially because surface water often has an evaporation signal [*Clark and Fritz*, 1997]. Several tracers cover different age-ranges for groundwater, including sulfur hexafluoride (SF$_6$), and tritium (^{3}H) for relatively young groundwaters (years to decades) and carbon-14 (^{14}C) and helium-4 (^{4}He) for older groundwaters (hundreds to >10,000 years). Sulfur hexafluoride concentrations have increased in the atmosphere since the 1960s due to anthropogenic inputs [*Plummer and Busenberg*, 2000]. Sulfur hexafluoride concentrations in groundwater reflect the air-water equilibrium concentration at the time of recharge, as well as the presence of excess air in groundwater from the dissolution of air bubbles trapped below a rising water table [*Aeschbach-Hertig et al.*, 1999]. Thus, for accurate SF$_6$ dating, correction for temperature at recharge and excess air entrapment in groundwater are required and usually estimated from noble gas concentrations [*Plummer and Busenberg*, 2000]. Tritium and ^{14}C are radionuclides with half-lives of 12.32 and 5730 years, respectively [*Clark and Fritz*, 1997]. They are both naturally produced in the upper atmosphere by cosmic rays but were also released in larger quantities in the 1950s and 1960s by atmospheric nuclear weapon testing [*Kalin*, 2000;
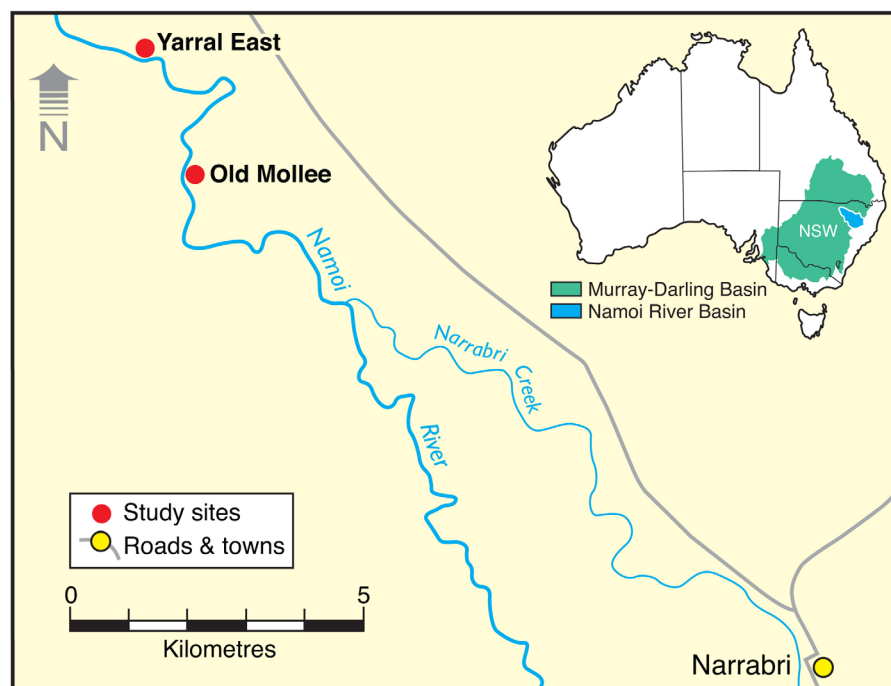
Figure 1. Location of the two piezometer transects (Yarral East and Old Mollee) downstream from Narrabri, NSW, and location of the Murray-Darling and Namoi River basins (inset).

Solomon and Cook, 2000]. However, at least in the Southern Hemisphere, the ^{3}H bomb peak is now almost gone having radioactively decayed or been dispersed away in water systems, and most of the ^{3}H in aquifers will be from natural sources [*Morgenstern et al.*, 2010; *Stewart et al.*, 2012]. The noble gas ^{4}He is an end-product of the alpha decay of thorium and uranium [*Solomon*, 2000]. Helium-4 gradually accumulates in pore water and is useful for dating old groundwater sources (generally ~1000 years and older) [*Bethke et al.*, 1999; *Mahara et al.*, 2009], but occasionally can be used in younger (50 years) groundwater as well [*Solomon et al.*, 1996].

The aim of this study was to evaluate groundwater-surface water interactions at the riparian scale (0–350 m) for an exploited, subtropical alluvial aquifer (Lower Namoi River, New South Wales, Australia). A particular emphasis was to evaluate if environmental age tracers can be used to estimate infiltration rates in this environment. The Lower Namoi Alluvium is one of the most heavily exploited groundwater resources in Australia, resulting in the Lower Namoi River having been a losing system for several decades prior to the study [*McCallum et al.*, 2013; *Lamontagne et al.*, 2014]. The initial conceptual model was for groundwater in the riparian zone to be river-derived, to have increasing Mean Residence Times (MRT) away from the river but, because of high infiltration rates, to remain relatively young (<30 years). In the following, the study area is described and the results of hydrometric monitoring and environmental tracer sampling during the study period (November 2009 to November 2011) are presented. This period covered the end of a regional drought followed by several high-flow events (that is, bank full or greater). Two additional tracers sampled (^{222}Rn and chlorofluorocarbons) are not further discussed here because their dating range was either too short to be useful (^{222}Rn) or were degraded in the aquifer (chlorofluorocarbons). However, the results for these tracers are provided in the supporting information.

2. Methods

2.1. Site Description

The Namoi River is a 40,000 km^2 catchment in northeast New South Wales, Australia (Figure 1). Climate is subtropical with a mean annual rainfall of 633 mm, generally higher in summer [*CSIRO*, 2007]. As for most other rivers in the Murray-Darling Basin (MDB), the Namoi River is heavily regulated by a system of reservoirs and weirs and part of an elaborate irrigation network. An extensive alluvial aquifer system occurs in
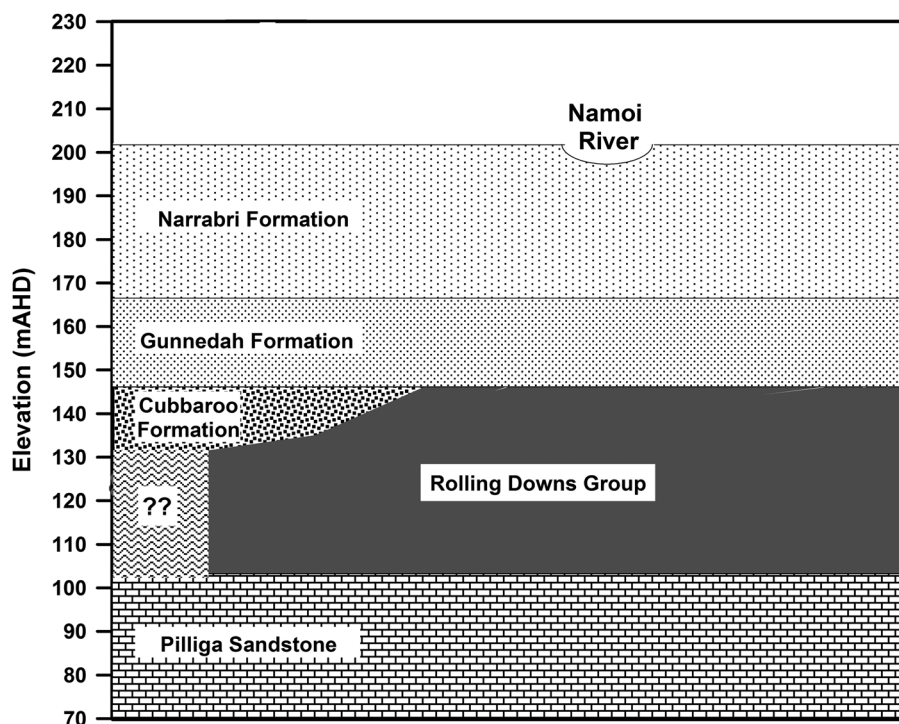
Figure 2. Simplified geological cross section of the Lower Namoi Alluvium and the upper Great Artesian Basin in the vicinity of the study area.

the Namoi Region and groundwater pumping accounts for 49% of water use, primarily for cotton irrigation. The study area is located in the Lower Namoi Alluvium approximately 12 km downstream of the town of Narrabri, and consists of two riparian piezometer transects (Old Mollee and Yarral East) approximately 2 km apart (Figure 1). The Lower Namoi Alluvium can be up to 120 m thick and consists of the shallow Narrabri Formation, the deeper Gunnedah Formation and, locally, a deeper paleochannel deposit (Cubbaroo Formation) [*CSIRO*, 2007]. The alluvium overlies the eastern edge of the Coonamble Embayment of the Great Artesian Basin (GAB) [*Smerdon et al.*, 2012] (Figure 2).

Each transect consisted of three pairs of nested piezometers and a surface water gauge (Figure 3). At each transect, one nest was installed as close to the river as practical (that is, on a river bench at Old Mollee and at the top of the bank at Yarral East) and the others up to 300 m further away in the floodplain. The downstream Yarral East was in a grazing paddock overlooking a steep bank, while Old Mollee was on a reserve (public park) with a more extensive coverage of riparian trees. In a nest, each piezometer was installed singly (that is, had its own hole) using cable tool drilling, which minimized the introduction of contaminants into the aquifer. The piezometers consisted of 95 mm diameter class 12 PVC in glued lengths, a 2 m length screen (1 mm slots), and a 1 m sump. The annulus was backfilled with waterworn rounded gravels, sealed with bentonite, and grouted to ground level. Each piezometer was protected at the surface by a 2 m lockable steel casing (in two 1 m sections) bolted into a cement base. At each nest, one screen was located ∼4–5 m and the other ∼10 m below the water table under base flow conditions. Below a silt veneer on the floodplain, the aquifer material was a mixture of sand and gravel units, with some clay at depth (Figure 3). The location of piezometers, surface water gauging stations, and a profile of the land surface and riverbed elevation were surveyed relative to the Australian Height Datum (AHD; similar to mean sea level).

2.2. Water Level and Piezometric Surface Monitoring
River stage and groundwater levels were monitored at 15 min intervals for various periods between March 2009 and November 2011 using unvented pressure transducers (Mini-Diver; Schlumberger Water Services). A barometric pressure logger with the same technical specifications was deployed in one of the piezometers at each transect to convert absolute pressures into hydraulic heads. The loggers were downloaded and
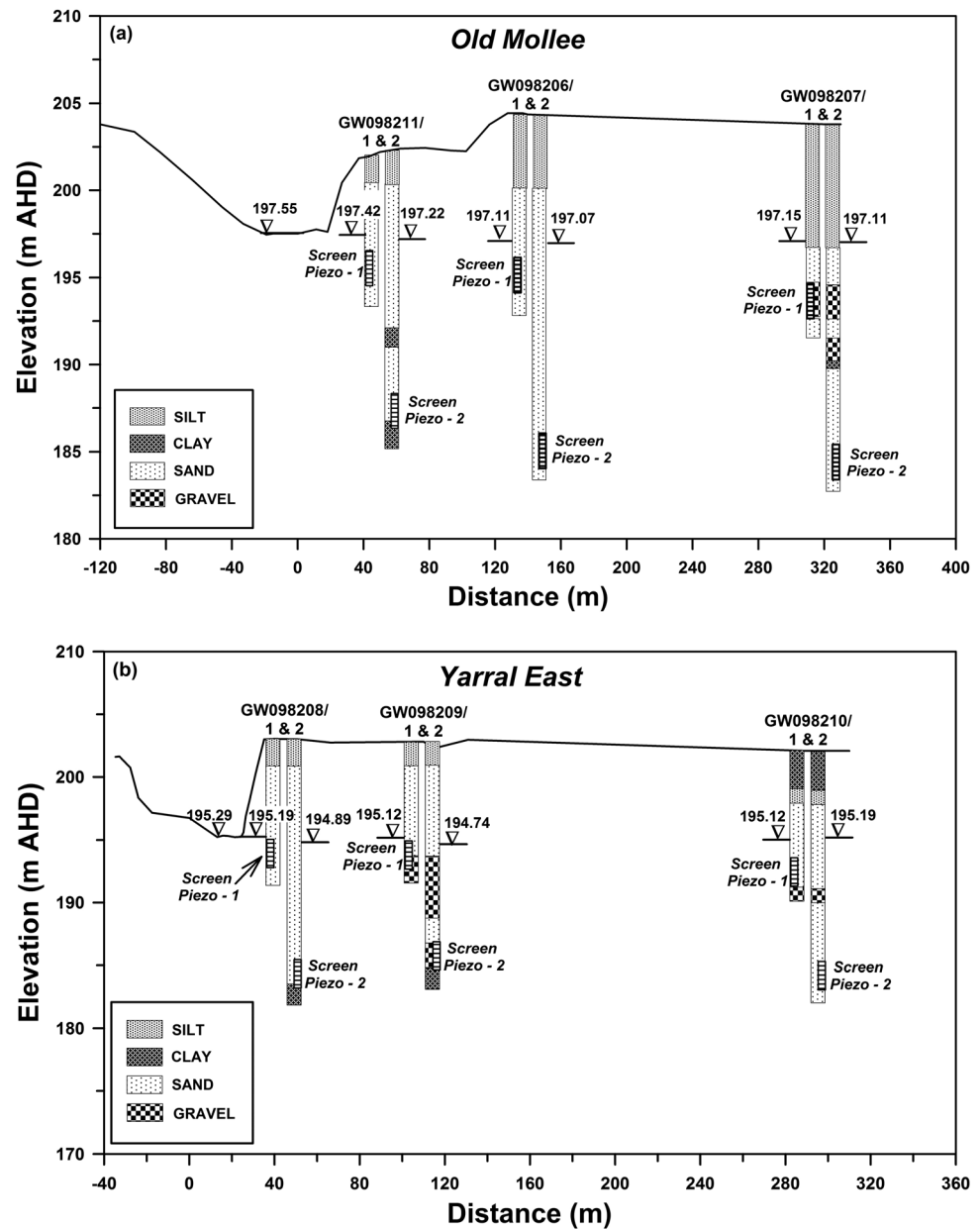
Figure 3. Cross section of the floodplain and river channel at the two piezometer transects. Also shown is the position of each piezometer screen, the water levels at November 2009, and the texture of aquifer material from borehole logs. At each piezometer nest, the water level on the left is for the deeper piezometer and the one on the right is for the shallower piezometer. Note that the piezometer nest closest to the river at Old Mollee is on a bench rather than on top of the bank.

water levels measured manually quarterly. While river stage was measured at both sites (Namoi River at Galatheria, NSW Station 419100 and Namoi River at Yarral East, NSW Station 419101), these stations were only operational between March 2009 and November 2009, after which they were damaged by a stormflow in January 2010. However, an existing river gauge was also present at Old Mollee (Namoi River at Old Mollee, NSW Station 419139) and has a continuous record. An estimate of river stage for Yarral East was obtained by adjusting stage at Station 419139 to the stage differences observed between Stations 419100 and 419101 (-2.1 m) when both were active. Groundwater levels were measured between March 2009 and March 2010 in all piezometers and, in selected piezometers, between March 2011 and November 2011. However, even within these periods, the record in some piezometers was incomplete due to equipment failure.

2.3. Environmental Tracer Sampling

Groundwater was sampled from the piezometer network on four occasions (November 2009, November 2010, April 2011, and November 2011). These corresponded to the end of a prolonged base flow period during a drought (November 2009), a bank full flow following drought-breaking rains (November 2010), a flow recession (April 2011), and another base flow period (November 2011; Figure 4a). On each sampling trip, manual water levels in each piezometer were taken before they were purged for three bore volumes. Special care was taken to locate the pump head at least 1 m above the top of the screen and to purge piezometers slowly to avoid dewatering at the screen level.

Electrical conductivity, pH, and temperature were measured in the field under flowing water using calibrated probes. Dissolved oxygen was also measured in the field using a Winkler titration test. For major ions and stable isotopes of water, water samples were 0.45 μm filtered in a field laboratory soon after collection. Stable isotope of water samples were stored inverted in a gas-tight collection vessel (McCartney bottle). For major cations, 50 mL samples were stored in well-rinsed PET bottles and acidified to pH < 2. For major anions, pH and alkalinity, filtered samples were stored in a similar fashion but without acidification. Water for SF_6 analysis was pumped through a nylon tube into 1 L amber glass jars filled from the bottom and allowed to overflow for 5 min. For noble gases, equilibrium head space samples were collected using passive diffusion samplers [Gardner and Solomon, 2009]. Diffusion samplers were allowed to equilibrate with sample water (i.e., immersed in the piezometer at screen level or in the river) for 24 h, retrieved and clamped vacuum tight. Water for ^3H and ^{14}C analyses was collected in 1 and 5 L polyethylene bottles, respectively. In addition to samples collected during the four sampling trips, between August 2010 and December 2011, weekly river samples were collected for chloride concentration and the stable isotopes of water at Narrabri (at the NSW river stage Station 419003).

2.4. Analytical Procedures

Laboratory electrical conductivity (Meterlab CDM 230) and pH were measured with calibrated probes in a constant temperature room. Total alkalinity was measured by titration to a pH 4.5 end point. Major cations were measured by Inductively Coupled Plasma Optical Emission Spectrometry (Spectro ARCOS) and anions by ion chromatography (Dionex ICS-2500). All major ion analyses were performed at the CSIRO Waite Campus Analytical Services Unit (Australia). The isotope ratios of water were measured by isotope ratio mass spectrometry (Europa Geo 20-20) using the Water Equilibration System (WES) technique or the uranium reduction method. The latter technique was used when the presence of H_2S in samples was suspected to interfere with the measurements of deuterium using the WES technique. The isotope ratios (R) were expressed in parts per thousands (‰) relative to Vienna Standard Mean Ocean Water (VSMOW) using the delta (δ) notation. For $^2H/^1H$

$$\delta^2H = \left[\frac{R_{sample}}{R_{standard}} - 1 \right] \cdot 1000 \qquad (1)$$

Neon-20, ^{40}Ar, N_2, and ^4He concentrations were measured using a quadrupole mass spectrometer with cryogenic separation [Poole et al., 1997] and concentrations expressed at standard temperature and pressure (STP). Measurement precision is approximately 5% for He, Ne, Ar close to solubility equilibrium and around 20% for He values higher than 20 times solubility equilibrium. Sulfur hexafluoride was analyzed using a head space method and electron capture gas chromatography, with a precision of 10% on repeated analyses and a detection limit of 0.2 fmol kg^{-1}. Stable isotope ratios, SF_6, and noble gas analyses were performed at the CSIRO Waite Campus Isotope Analysis Service (IAS). Reproducibility of the IAS noble gas and SF_6 analyses was recently found to be similar to the one of other laboratories as a part of an intercomparison study [Labasque et al., 2014; Visser et al., 2014]. Carbon-14 was measured by accelerator mass spectrometry at the SSAMS Radiocarbon Dating Centre, The Australian National University, following Fallon et al. [2010]. Carbon-14 results are expressed in percent modern carbon (pmC; the ^{14}C activity for CO_2 in 1950, prior to atmospheric thermonuclear testing) without correction for water-rock interactions. Tritium activities were measured at the GNS Laboratory (New Zealand) following electrolytic enrichment [Morgenstern and Taylor, 2009], with a detection limit of 0.02 TU and a precision at an average ^3H concentration of recent rain of ± 0.04 TU. Rainfall ^3H in the Namoi catchment is 2.4–2.8 TU [Tadros et al., 2014].
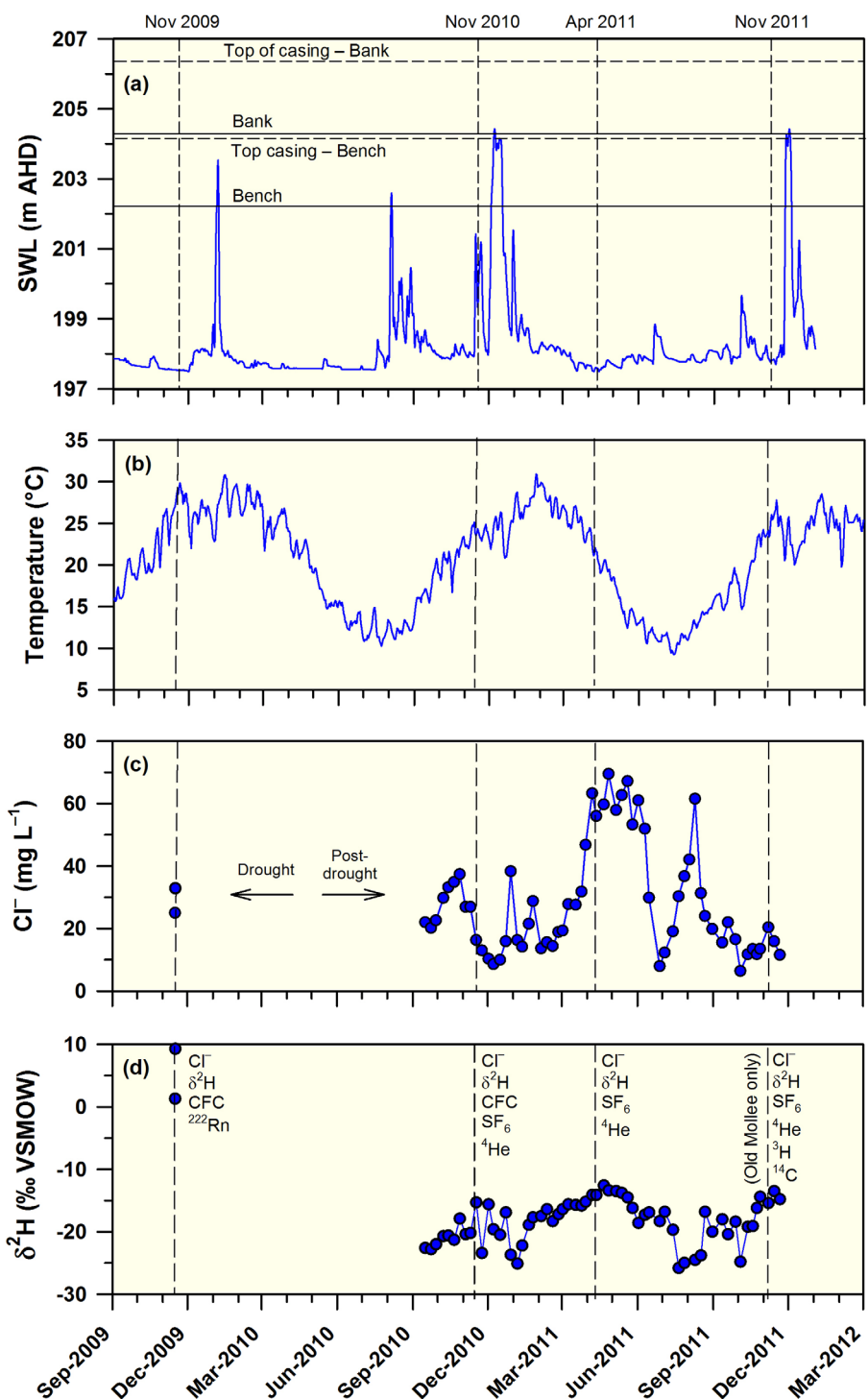
Figure 4. Variations in (a) river stage (NSW Station 419039), (b) temperature, (c) chloride concentration, and (d) δ^2H in the Namoi River during the study period. Vertical dotted lines indicate each sampling period. The horizontal lines in Figure 4a represent the elevation at the base or top of the piezometer casing at the bench or at the bank at Old Mollee (note that there were no bench piezometers at Yarral East). Which tracers were sampled for each sampling campaign are shown in Figure 4d.

2.5. Lumped Parameter Models

The calibration of SF_6 dating with ^{3}H, the degree of mixing, and the variations in Mean Residence Time (MRT) of groundwater in the riparian zone were evaluated using lumped parameter models (LPM). Briefly, lumped parameter models convolute an input function for a tracer into an aquifer (such as the variations in

[14]C fallout from the atmosphere over time) to an output after passage through the aquifer using an idealized representation of the age-distribution in groundwater samples [*Vogel*, 1967; *Cook and Böhlke*, 2000]. These can be compared using different formulations for the convolution integral

$$C_{out}(t) = \int_{-\infty}^{t} C_{in}(t') \cdot g(t-t') \cdot e^{-\lambda(t-t')} dt' \qquad (2)$$

where $C_{in}(t)$ is the input function for the tracer, $C_{out}(t')$ the concentration in the aquifer at different times, $g(t-t')$ the age distribution describing the relative contribution of water with a certain age $(t-t')$ within a mixed sample, and $e^{-\lambda(t-t')}$ is radioactive decay. In the simplest cases of the Piston Flow Model (PM) and the Linear Model (LM), the groundwater sample is assumed to have a unique source and age or a constant age distribution over a defined period, respectively. In more complex cases, like the Exponential Model (EM) and the Gamma Model (GM), the groundwater sample is assumed to include water from a range of sources each with its own age [*Maloszewski and Zuber*, 1982; *Kirchner et al.*, 2000]. The main advantages of lumped parameter models over more complex numerical solute transport models are that they are nondimensional and few parameters need to be fitted. However, lumped parameter models assume that flow is constant and that the underlying age-distribution of groundwater is known.

Here we also use the more flexible Dispersion Model (DM) to explore the properties of the aquifer. The DM is similar to the advection-dispersion solute transport model. The parameters to be fitted are MRT and the Peclet number (*Pe*; the ratio of advective to dispersive transport in the aquifer). The PF and EM are special cases of the DM where the Peclet number is either very large or very small, respectively. The input functions for the tracers were measured at Cape Grim (Tasmania, Australia) for SF_6, Kaitoke, and Wellington (New Zealand) for southern hemisphere ^{3}H and ^{14}C, respectively. All these input functions were evaluated as annual mean concentrations, and to all these input functions correction factors were applied that will be explained in detail in the Discussion. All computational analyses were performed using the software Lumpy [*Suckow*, 2012]. The effects of variations in recharge temperature and excess air on SF_6 concentrations in the aquifer were evaluated by comparing SF_6 and ^{3}H concentrations (the latter tracer not being affected by variations in recharge temperature or in excess air).

3. Results

A large environmental tracer database was assembled during the project, which is only summarized in the following. Interested readers can consult the complete database in the supporting information.

3.1. Hydrometry

The four sampling periods for riparian groundwater represented the different hydrological conditions observed during the study period. The first sampling (November 2009) occurred at the end of a regional drought in southeastern Australia (Figure 4a). At that time, the river was flowing gently at the upstream site (Old Mollee) but was a series of disconnected pools at the downstream one (Yarral East). Following drought-breaking rains in 2010, several high-flows occurred between August 2010 and March 2011. Flows were within the river banks but at least one (December 2010) overtopped the banks. The first of the two larger flows (August 2010) occurred during winter, when water temperatures were colder (Figure 4b). Most piezometers would have had their bases covered with water by the December 2010 event but they were not overtopped, with perhaps the exception of the piezometer nest on the river bench at Old Mollee for a short period of time (GW098211; Figure 3). Note that piezometers extended 1 m above the ground surface and that their protective casings extended 2 m above the ground surface. Thus, it is unlikely that piezometers were contaminated during higher flows.

3.2. Weekly River Water Quality Monitoring

River water quality varied during the study period as a function of the hydrograph and antecedent conditions. Chloride concentrations varied in accordance with the hydrograph, with the highest values (60–70 mg L^{-1}) observed during flow recession (Figure 4c). At the end of the drought, river water was enriched in heavier stable isotopes (Figure 4d). In November 2009, δ^2H was 1.3‰ at Old Mollee and 9.9‰ at Yarral East. These elevated values were the result of evaporative enrichment following long residence times
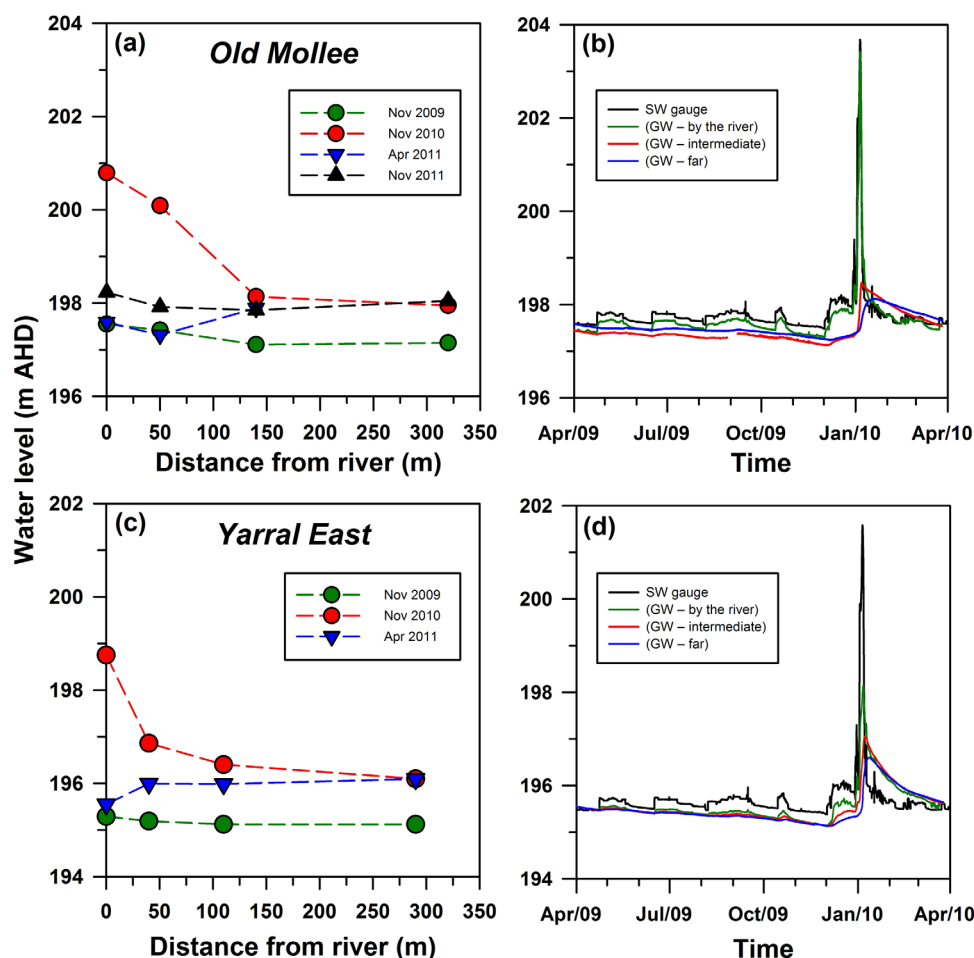
Figure 5. Examples of gaining and losing conditions at the scale of the riparian zone. Water table elevation at (a) Old Mollee and (c) Yarral East during the four sampling campaigns (river stage is at distance = 0 m). Hydraulic head in shallow piezometers between April 2009 and April 2010, showing the water table response during managed flow releases (2009) and a natural floodwave (2010) at (b) Old Mollee and (d) Yarral East.

in the river and upstream reservoirs, releases from which were providing the base flow at that time. Post drought, river δ^2H values fluctuated between -26 and $-17‰$, with the highest values observed during flow recession. While there was no systematic difference in river Cl$^-$ concentration during and after the drought, river water was isotopically enriched during the drought.

3.3. Riparian Water Table Fluctuations

Based on the shallowest piezometer at each nest, the position of the water table varied as a function of antecedent conditions and the river hydrograph. In November 2009 (during the drought), the water table was relatively low and the river was losing to the riparian zone (Figures 5a and 5c). Post drought, the water table increased by at least ~1 m. In November 2010 (rising phase of the hydrograph), the river was strongly losing while in April 2011 (flow recession) it was gaining. In November 2011 (base flow), the river was losing again. The patterns were similar at the two transects but at Old Mollee during base flow conditions (November 2009 and November 2011) the water table was lowest at intermediate distances. This probably reflected groundwater transpiration by the mature riparian trees lining the river banks at Old Mollee (with Yarral East lacking a similar riparian cover). Overall, while the river was generally losing, high-flows could generate gaining conditions from bank discharge for weeks to possibly months during flow recession (Figures 5b and 5d). However, smaller managed flow releases during low-flow conditions did not generate bank-discharge cycles, probably because of flatter floodwave profiles relative to unregulated high-flows (see several examples between April and November 2009 in Figures 5b and 5d). The increase in water table level
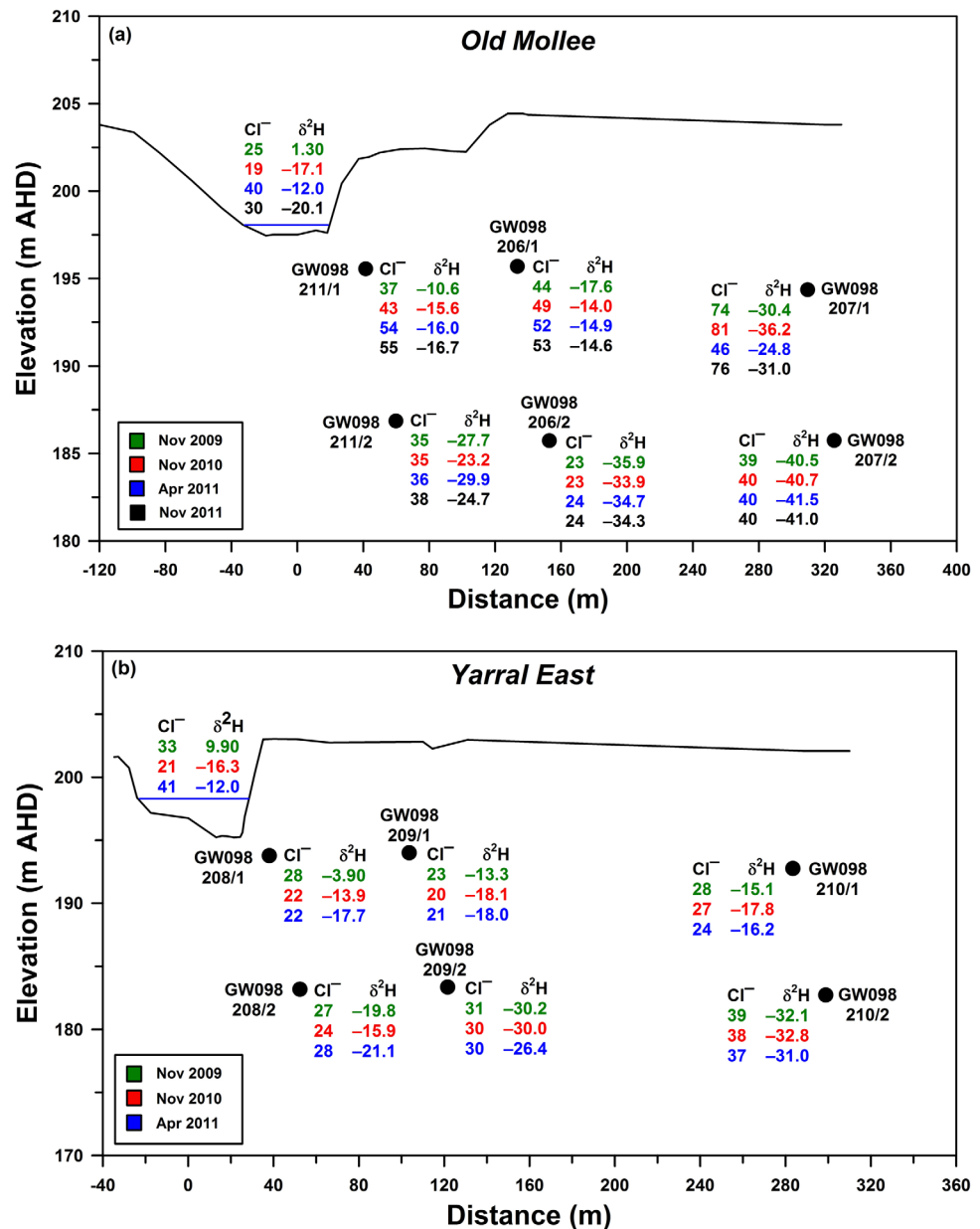
Figure 6. Chloride concentration (mg L^{-1}) and δ^2H (‰ VSMOW) during the four sampling campaigns (there was no sampling at Yarral East on November 2011). (a) Old Mollee and (b) Yarral East.

observed between November 2009 and November 2010 suggests a significant recharge of riparian groundwater during 2010.

3.4. Groundwater Cl$^-$, δ^2H, and δ^{18}O

The trends in Cl$^-$, δ^2H, and δ^{18}O suggested that riparian groundwater had two different sources. For example, at Old Mollee, groundwater δ^2H values ranged from -10.6‰ close to the river to -41‰ deeper and farther away (Figure 6). Near the river, δ^2H became lower over time (Figure 6). Variations in Cl$^-$ concentrations were not as pronounced, with a trend towards higher values away from the river. Examination of δ^{18}O and δ^2H for all surface and groundwater samples showed that river water was enriched in the heavier isotopes, was more variable, and occasionally had an evaporation signal (that is, was relatively more enriched in δ^{18}O relative to δ^2H as compared to the meteoric water line; Figure 7). The source for river water (that is,
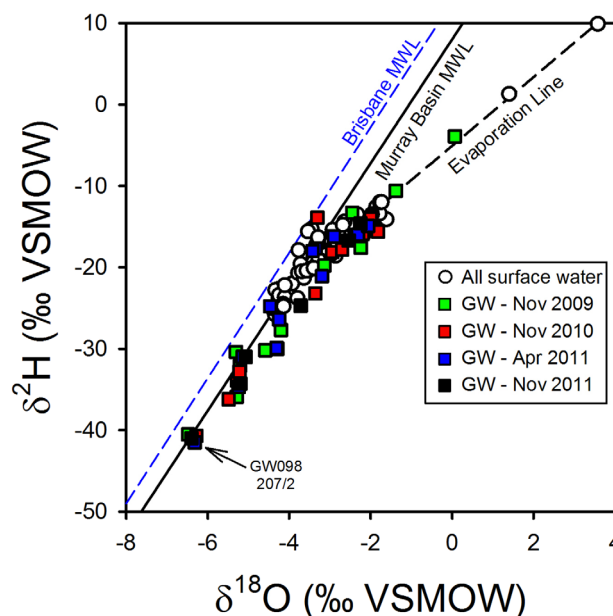
Figure 7. δ^2H-δ^{18}O plot for all surface and groundwater samples collected during the study. Also shown is the Brisbane Meteoric Water Line (δ^2H = 7.6·δ^{18}O + 13) [*Crosbie et al.*, 2012], the Murray Basin Meteoric Water Line (δ^2H = 7.6·δ^{18}O + 8) [*Simpson and Herczeg*, 1991] and the evaporation line for the surface water samples (δ^2H = 4.3·δ^{18}O − 5.1).

where the river water evaporation line intersects with the Murray Basin Meteoric Water Line; Figure 7) had a signature of δ^2H = −21‰ and δ^{18}O = −4.0‰. In contrast, one of the deepest piezometers (GW098207/2) had an isotopically depleted signature which remained constant over time (δ^2H = −41‰ and δ^{18}O = −6.4‰). None of the river water samples collected during the study period had such a depleted signature, so this probably represents a source of water other than surface water (hereafter referred to as "regional groundwater"). Aside from GW098207/2, all other groundwater samples could be a mixture between a river and regional groundwater end-member. Thus, at the scale of the riparian zone, mixing of different groundwater sources was significant.

3.5. SF$_6$, Ar, and Ne
Sulfur hexafluoride concentrations in riparian groundwater ranged from near detection limit (0.22 fmol kg^{-1}) in some of the deeper piezometers, 1.6–2.0 fmol kg^{-1} in the river, and up to 3.9 fmol kg^{-1} in groundwater closest to the river (Figure 8). At both sites, the highest SF$_6$ concentrations were found at the shallowest piezometer next to the river and declined over time (Figure 8). For example, at Old Mollee GW098211/1, SF$_6$ concentration was 3.9 fmol kg^{-1} in November 2010, 3.3 fmol kg^{-1} in April 2011, and 2.2 and 3.0 fmol kg^{-1} in duplicate samples taken in November 2011. A similar pattern was observed at Yarral East, but the SF$_6$ concentration gradient was smaller. Extremely high values recorded in one deep piezometer in November 2011 (4.2 and 6.7 fmol kg^{-1}) may be a contamination artifact during sampling, especially considering concentrations at that piezometer were much lower on previous sampling dates (0.43 and 0.85 fmol kg^{-1}). The SF$_6$ concentrations in the river are close to the expected equilibrium with the atmosphere for the Southern Hemisphere (around 7 pptv for the Southern Hemisphere in 2011). Thus, the higher SF$_6$ concentrations in shallow groundwater suggest that the source of water there had some excess air or a lower temperature at the time of recharge, both of which can increase dissolved SF$_6$ concentrations.

Trends in groundwater Ne and Ar concentrations were used to evaluate whether lower-than-anticipated recharge temperatures or the presence of excess air in groundwater could account for SF$_6$ concentrations above expected equilibrium with the atmosphere. The average annual air temperature at Narrabri, a proxy for recharge temperature, is 19°C (http://www.bom.gov.au/climate/averages/tables/cw_053030.shtml). This is consistent with groundwater temperatures at the time of sampling, which ranged between 17 and 23°C (supporting information). However, Namoi River temperatures vary between 10 and 30°C on an annual basis (Figure 4b), with a tendency for colder temperatures during winter and during significant flows. In addition, the break of the drought was associated with a large winter flow. Thus, the potential exists for infiltration of water colder than 19°C in the months preceding the first sampling for SF$_6$ (November 2010). The trends in groundwater Ne and Ar concentrations show the presence of moderate to high amounts of excess air in riparian groundwater (0–0.005 cm^3 STP g^{-1}) and that recharge temperatures could have varied between 9 and 20°C (Figure 9). Some of the surface water samples were depleted in Ne (data to the left of the Ne-Ar equilibrium solubility line). This probably represented imperfect equilibrium between the diffusers used to collect the samples and ambient surface water, generated by diurnal variations in water temperature in the river. Thus, a combination of low temperature at the time of infiltration and some excess air in alluvial groundwater could account for the elevated SF$_6$ concentrations in shallow riparian groundwater (see further analysis in section 4.1).

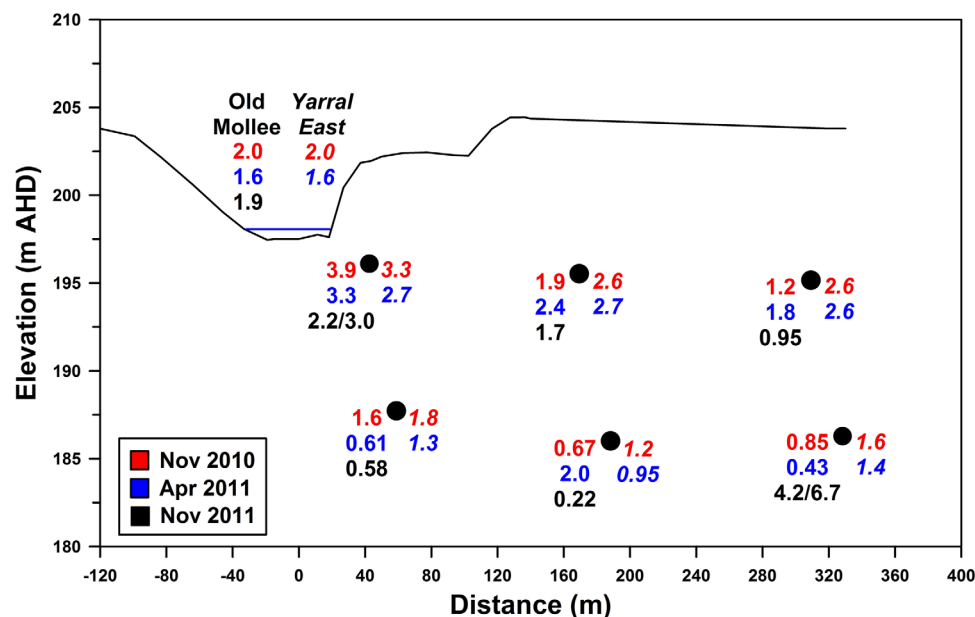**Figure 8.** SF_6 concentrations (fmol kg^{-1}) in surface and groundwater at Old Mollee and Yarral East on three different sampling campaigns (cross section for Old Mollee shown).

3.6. Carbon-14, ^{3}H, and ^{4}He

The patterns in ^{3}H activity in groundwater were similar to those of SF_6 (Figure 10) with the highest activities in the piezometers closest to the river (2.08 ± 0.041 TU at GW098211/1), slightly lower than river water (2.41 ± 0.048 TU), and the lowest activities away from it (−0.005 ± 0.015 TU at GW098207/2). Thus, a high proportion of relatively young groundwater (with ages of years to decades) was present in the shallower piezometers. This was consistent with modern ^{14}C values (100–104 pmC) in groundwater from the shallower piezometers (Figure 10). Helium-4 concentration in solubility equilibrium with river water is expected to be 4.1–4.5 × 10^{-8} cm^3 STP g^{-1} between 10 and 30°C. However, elevated ^{4}He concentrations were found in deeper piezometers in November 2010 (supporting information), April 2010 (supporting information), and in November 2011 (Figure 10). Helium-4 concentrations were close to equilibrium with the atmosphere in the river and in most shallow piezometers (4.5–10 × 10^{-8} cm^3 STP g^{-1}), but greater than 2000 × 10^{-8} cm^3 STP g^{-1} in some of the deeper piezometers (Figure 10). Groundwater with elevated ^{4}He also tended to have less than modern ^{14}C values (Figure 10). For example at GW098207/2 in November 2011, the ^{4}He concentration was 2100 × 10^{-8} cm^3 STP g^{-1} and the ^{14}C activity 30.4 pmC. Based on ^{14}C and ^{4}He, the origin of groundwater with a low δ^2H found in the riparian zone was probably significantly older than currently infiltrating river water (possibly by millennia).

4. Discussion

Alluvial aquifers are among the most heavily exploited groundwater resources and there is considerable interest to understand their connectivity with rivers [*Brunner et al.*, 2009; *Eastoe et al.*, 2010; *Lamontagne et al.*, 2014]. Infiltration processes can often only be approximately represented in regional groundwater models [*Brunner et al.*, 2010; *Rassam*, 2011], and key system properties, like the hydraulic conductivity of the riverbed, are usually not known [*Rassam et al.*, 2008]. Thus, independent estimates of river infiltration rates may improve the calibration of the models used to manage alluvial groundwater resources. Here a section of the Namoi River was instrumented with a purpose-built riparian piezometer network to evaluate if environmental age tracers can be used to provide an independent estimate of infiltration rates in exploited subtropical aquifers. The piezometer spacing (tens to hundreds of meters) was designed for estimating infiltration rates with "young" groundwater tracers (chlorofluorocarbons, SF_6, tritium, and the "bomb" component of ^{14}C). In general, the patterns in the "young" groundwater tracers were consistent with a losing river environment, suggesting that these tracers could be used to estimate infiltration rates. In practice, the
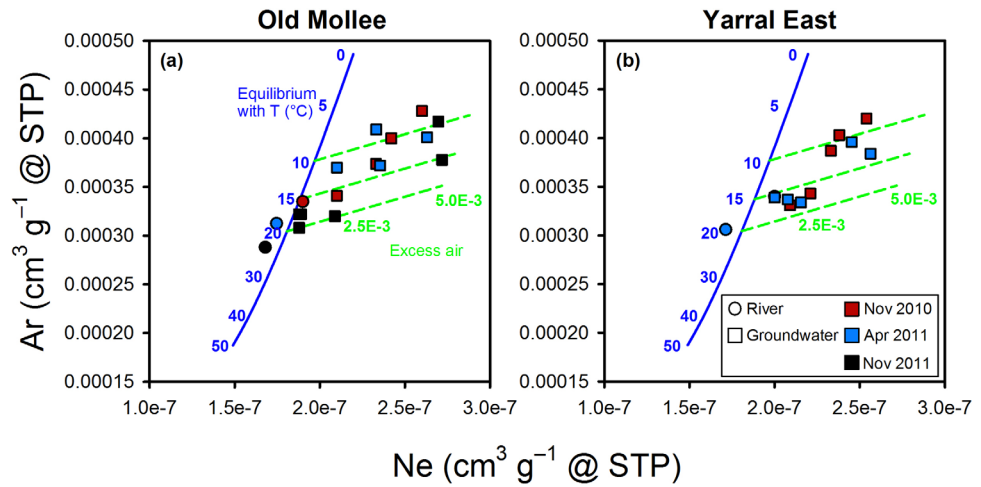
Figure 9. Ne and Ar concentrations in surface and groundwater samples on three sampling campaigns for (a) Old Mollee and (b) Yarral East. Also shown are the expected equilibrium concentrations relative to their temperatures (blue line) and excess air contents (green line; cm^3 STP g^{-1}).

combination of a dynamic hydrological environment and the presence of more than one groundwater source at the scale of the riparian zone complicated the interpretation of the tracers significantly. In the following, this will be demonstrated by using lumped parameter models to estimate a preliminary range in infiltration rates. In addition, the evidence for a significant episodic recharge event during the study is reviewed and the origin of the "old" groundwater source in the riparian zone is further discussed.

4.1. Lumped Parameter Models

To estimate infiltration rates, tracer concentrations were modeled into apparent ages using lumped parameter models. When applying environmental age tracers to infiltration from river water, the input function for all tracers is never known precisely. Tritium records in precipitation are usually not measured in the investigated catchment. Variations in precipitation from one area to another can be approximated by applying a
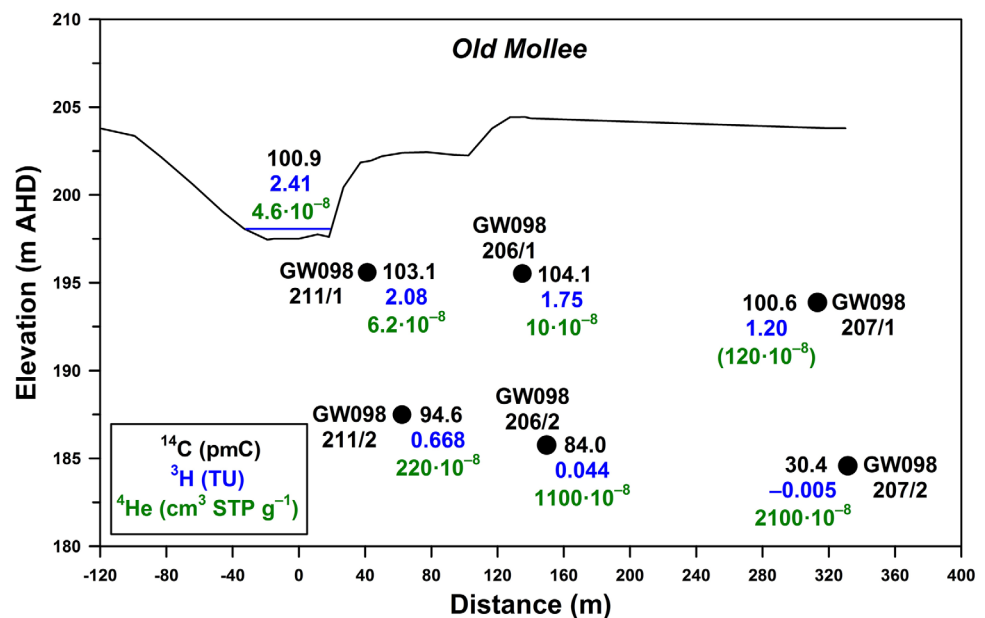

Figure 10. Carbon-14, ^{3}H, and ^{4}He concentrations at Old Mollee on November 2011, except for ^{4}He at bore GW098207/1 which was the average from the November 2010 and April 2011 samplings.

correction factor to the tritium input curve, accounting for the continental effect [*Tadros et al.*, 2014]. The river system itself can have a mean residence time of months to years [*Aggarwal et al.*, 2010], which can be accounted for if a tritium time series is available. Because no such time series is available for the Namoi River, here the mean residence time was assumed to be comparably short and constant. Carbon-14 in atmospheric CO_2 needs to be translated into ^{14}C in total dissolved inorganic carbon (TDIC) of river water or groundwater to take into account the input of "dead" ^{14}C by carbonate dissolution. This can be accomplished by using a correction factor <1, and this factor may vary with time if the geochemical environment is not constant. Furthermore, SF_6 concentrations will be influenced by temperature of the river water and by excess air generated when the river water infiltrates. Both processes together can change the resulting SF_6 concentration by a factor of two. Lastly, many piezometers (especially the deeper ones) appeared a mixture between an old and a young groundwater source. This mixture must be quantified to estimate an MRT for each source. Here a stepwise approach was used to evaluate the influence of these factors for each tracer.

In a first step, the correction factors needed to adapt the ^3H and ^{14}C input functions for river water were evaluated. The surface water sample was best described using a correction factor of 1.25 on the ^3H input curve. This is reasonable in view of a higher continental influence of the Namoi catchment as compared to Kaitoke where the record originates [*Tadros et al.*, 2014]. All tested models (that is, PM, EM, DM, LM, and GM) were in agreement for surface water being diluted by a factor of 0.96 in ^{14}C activity relative to the atmospheric record. Using the adjustments to the ^3H and ^{14}C input functions, the river water sample could be fitted with an MRT of less than a year in all LPM (Figure 11a). However, no LPM could simultaneously fit all measured groundwater samples in the $^3H/^{14}C$ parameter space (Figures 11a and 11b). More specifically, all models could provide a reasonable fit to the shallow groundwater samples but none could fit the deeper samples. The best fitting model for all samples was the Dispersion Model with $Pe = 0.1$ (Figure 11b), consistent with an environment where solute dispersion is important. The inference from these patterns is that two flow systems were present: a shallow one mostly containing infiltrated river water moving away from the river and a deeper one containing various mixtures of young and old groundwater.

In the next step, the Dispersion Model was used to evaluate the environmental controls on tracer concentrations in the aquifer. While not providing a universal fit, the DM is easier to interpret and was thought to reasonably represent the process of solute transport, at least for the shallow samples. Dispersion models with a range in Pe (0.1–5) were tested and a reasonable fit was obtained for $Pe \sim 0.1$ for most of the ^3H and ^{14}C data (Figure 11b). However, GW098207/1 and −211/2 had lower ^{14}C values than all model curves and GW098211/1 had a higher ^{14}C value than all curves. One possibility to explain this finding is that the factor 0.96 applied to translate the atmospheric ^{14}C input function into TDIC ^{14}C values in water is not constant as was assumed here. For the same range in Pe, all $^3H/^{14}C$ samples can be accounted for when the ^{14}C input function correction factor ranges between 0.91 and 0.97 (Figure 11c). When combining both the uncertainty in Pe and ^{14}C input function, a comparably wide range in MRT is found for each piezometer (Table 1). Peak Transition Ages (t_{peak}) were also estimated for the $^3H/^{14}C$ samples because this metric is potentially a better indicator of transit times when solute transport is highly influenced by dispersion [*Weissman et al.*, 2002] and can be estimated from

$$t_{peak} = \frac{MRT}{Pe}\left(\sqrt{9+Pe^2}-3\right) \qquad (3)$$

The t_{peak} range for the $^3H/^{14}C$ samples was also wide but different than the MRT range (Table 1). For example, for GW098211/1, MRT was 4–12 years and t_{peak} was 0.07–1.9 years. Alternative dispersion models combining SF_6 and ^3H were used to attempt to narrow the MRT or t_{peak} range estimated for each piezometer. However, the main influence factor on SF_6 concentration is temperature and excess air (Figure 11d), so the uncertainty in MRT or t_{peak} could not be reduced. Dispersion and mixing processes in the riparian zone may be too complex to be accurately represented by LPM, but the MRT and t_{peak} obtained are a starting point to estimate a likely range in infiltration rates. Below, the magnitude of the infiltration rate is estimated using the range in MRT and t_{peak} estimated using the Dispersion Model with $Pe = 0.1–1$.

4.2. Infiltration Rates

In losing-connected aquifers, net recharge is often less than infiltration because a part of the water infiltrated during flow pulses eventually returns to the river [*Freeze and Cherry*, 1979; *Vázquez-Suñé et al.*, 2007].
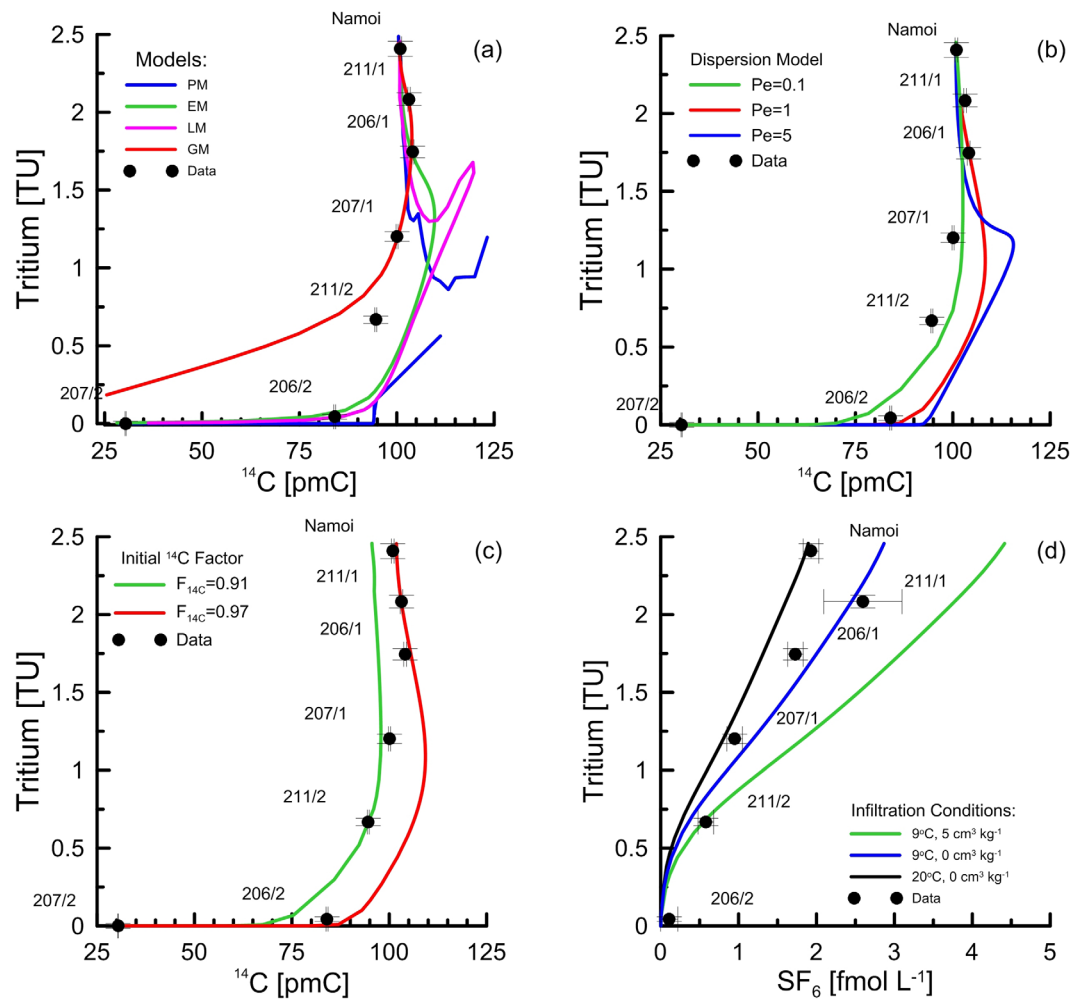
Figure 11. Evaluation of the ^{3}H, ^{14}C, and SF$_6$ data using lumped parameter models. (a) Comparison of different types of ^{3}H/^{14}C models (PM, Piston Flow; EM, Exponential; LM, Linear; GM, Gamma) [*Suckow*, 2012], (b) ^{3}H/^{14}C dispersion models for different Pe values, (c) Effects of variations in the ^{14}C atmospheric input function correction factor (F_{14C}) for a DM model with $Pe = 0.1$ (green) and 1 (red), and (d) SF$_6$ concentrations evaluated with a ^{3}H/SF$_6$ Dispersion Model with $Pe = 0.5$, showing that the range in excess air and in temperature at recharge estimated for the aquifer can account for the observed variations in SF$_6$ concentrations in shallow piezometers.

Here we compare instantaneous Darcy-derived minimum (q_{min}) and maximum (q_{max}) horizontal infiltration rates to the longer-term ^{3}H/^{14}C-derived mean horizontal infiltration rate to evaluate the contribution of low and high-flows to recharge at the Old Mollee site. Using the Dupuit-Forchheimer approximation [*Freeze and Cherry*, 1979], Darcy infiltration rates were evaluated using

Table 1. Infiltration Rates at Old Mollee Inferred From ^{3}H/^{14}C Dating Using Dispersion Models With Pe Varying Between 0.1 and 1 and an Atmospheric ^{14}C Input Function Correction Factor of 0.94[a]

Location	d (m)	MRT (years)	t_{peak} (years)	q_{mrt} (m yr^{-1})	q_{peak} (m yr^{-1})
Namoi River	0	0.1–1	0.002–0.16		
GW098211/1	44	4–12	0.07–1.9	1.2–3.4	7.4–200
GW098206/1	135	9–43	0.15–7.0	0.96–4.6	5.9–270
GW098207/1	330	32–170	0.53–28	0.59–3.1	3.6–190
GW098211/2	10[b]	115–700	1.9–114	0.004–0.027	0.27–1.6
GW098206/2	10[b]	>500	>110		
GW098207/2	9[b]	undef., >6 ky	>3000		

[a]All piezometer-specific q_{mrt} and q_{peak} are relative to distance from and MRT for (or t_{peak}) the Namoi River, except for GW098211/2 where the comparison is relative to GW098211/1 to evaluate the vertical infiltration rate.
[b]Midscreen distance below the upper piezometer in the nest.

$$q = -K \cdot i \tag{4}$$

where K is the hydraulic conductivity and i the hydraulic gradient between two riparian piezometers or between a piezometer and the river. The average K of the Namoi riverbed estimated by permeametry is 4×10^{-4} m s^{-1} [*Taylor et al.*, 2013]. In the shallow piezometers, the hydraulic gradients observed in the Old Mollee riparian zone were -0.003 to -0.00001 following prolonged low-flows and -0.02 to -0.01 during rising stages of the hydrograph. Thus, the horizontal q_{min} and q_{max} could range from 0.13 to 38 and 130 to 250 m yr^{-1}, respectively. For ^{3}H/^{14}C-derived mean infiltration rates

$$q_{mrt} = \frac{d_2 - d_1}{MRT_2 - MRT_1} n \tag{5}$$

where d_1 and d_2 are the distance from the river at two measurement points, MRT_1 and MRT_2 are the mean residence times at the two measurement points, and n is the porosity of the aquifer (assumed to be ~ 0.3 here). However, when dispersion is significant in the aquifer, the breakthrough curve for a tracer will have a trailing tail and the MRT may not be the best estimate for the average travel time of water [*Weissman et al.*, 2002]. When dispersion is significant, t_{peak} could provide a better estimate of infiltration rate (q_{peak}):

$$q_{peak} = \frac{d_2 - d_1}{t_{peak2} - t_{peak1}} n \tag{6}$$

For the shallow piezometers, the ^{3}H/^{14}C-derived MRT corresponded to horizontal q_{mrt} ranging from 0.59 to 4.6 m yr^{-1} (Table 1). However, horizontal q_{peak} was generally greater than horizontal q_{mrt}, ranging from 3.6 to 270 m yr^{-1} (Table 1). Vertical infiltration rates were more difficult to estimate because the MRT and t_{peak} in deeper samples were often extending beyond the age-range of the tracers (Table 1). However, for piezometer nest GW098211 (the one closest to the river), the range in vertical q_{mrt} and q_{peak} was 0.004–0.027 m yr^{-1} and 0.27–1.6 m yr^{-1}, respectively. A more detailed hydraulic analysis is not possible here because the riparian piezometer hydraulic head monitoring was short (~ 2 years) relative to the time scale represented by the tracers (up to decades). Overall, ^{3}H/^{14}C-derived horizontal infiltration rates at Old Mollee were within the range expected for q_{min} but could also represent a mixture of low and high-flow infiltration, as previously suggested for the Namoi River [*McCallum et al.*, 2014]. Infiltration rates for the Lower Namoi Alluvium are at the lower end of tracer-derived infiltration rates for exploited temperate alluvial aquifers (25–1700 m yr^{-1}) [*Bertin and Bourg*, 1994; *Beyerle et al.*, 1999; *Hoehn and von Gunten*, 1989]. This may be due, in part, to the seasonal use of groundwater from the Lower Namoi Alluvium and less reliance on groundwater for irrigation when not in drought.

4.3. Episodic Recharge

The piezometer network was sampled on several occasions for SF$_6$ because the elevated concentrations found in the piezometers next to the river (GW098211/1 at Old Mollee and GW098208/1 at Yarral East) in November 2010 initially appeared unlikely. However, SF$_6$ concentrations remained elevated in these piezometers over the next 2 years, showing that the trend was not an artifact. Noble gases and lumped parameter modeling both demonstrated that the elevated SF$_6$ concentrations could be accounted for by a combination of a lower than anticipated temperature at recharge and the presence of some excess air in groundwater. Temperature at recharge is usually assumed to be similar to the mean average air temperature when it occurs through a deep unsaturated zone [*Stute and Schlosser*, 1993]. While at the time of sampling riparian groundwater had a fairly narrow temperature range (17–23°C) close to mean annual air temperature (19°C), trends in noble gas concentrations suggested that temperature at infiltration varied between 9 and 20°C. This discrepancy between measured and inferred temperatures can be attributed to the tendency for oscillations in temperature in infiltrating water to rapidly dissipate in aquifers [*Constantz*, 2008; *Kulongoski and Izbicki*, 2008]. Thus, the most likely explanation for the pattern in SF$_6$ concentration is for one large winter river infiltration event occurring in winter 2010, ahead of the first sampling for SF$_6$. This also corresponds to a period when the water table rose by 1 m in the riparian zone. Episodic recharge can be anticipated for exploited semiarid and subtropical aquifers where drought and pumping can significantly depress the water table in the vicinity of rivers [*McCallum et al.*, 2013; *Lamontagne et al.*, 2014].

No attempt was made to estimate groundwater MRT with SF$_6$ because of the difficulties to calibrate concentrations relative to both excess air content and recharge temperature. The estimation of excess air and in

particular temperature used here should be interpreted with caution because only the light noble gases He, Ne, and Ar were measured, whereas the heavier noble gases Kr and Xe are more responsive to temperature variations [*Beyerle et al.*, 1999]. In addition, only one simple model for equilibration with excess air was used (total dissolution) [*Aeschbach-Hertig et al.*, 2000], whereas the dynamics of excess air in alluvial environments are unknown and are probably more complex, including partial dissolution and fractionation [*Aeschbach-Hertig et al.*, 1999; *Stute et al.*, 1995] and would require further investigation. Despite these difficulties, SF_6 still provided useful hints about the recharge environment at the sites. As SF_6 concentrations in the atmosphere are expected to keep increasing in the foreseeable future [*Maiss and Levin*, 1994; *Maiss and Brenninkmeijer*, 1998], it is worth persisting with this tracer as its signal in groundwater will increase and could become easier to interpret.

4.4. Origin of the Older Groundwater Source

The identification of an "old" source of groundwater in the riparian zone was not anticipated because it was believed that infiltration rates were large along this section of the Namoi River. However, while currently losing, the Lower Namoi River was gaining prior to a significant increase in groundwater extraction from the alluvium [*CSIRO*, 2007; *McCallum et al.*, 2013]. Thus, the older riparian groundwater source could be remnant alluvial groundwater derived by rainfall recharge in the floodplain from a period when the river was still gaining. However, because of the high ^{4}He concentrations found, the source for the older groundwater could also be leakage from the underlying Surat Basin of the Great Artesian Basin (GAB), a large confined regional aquifer of east-central Australia. In the vicinity of the study area, the GAB Pilliga Sandstone has artesian conditions and, moreover, could have partially eroded confining beds [*Smerdon et al.*, 2012]. The study area is also close to GAB intake beds, where "rejected recharge" can also contribute to river base flow [*Herczeg*, 2008]. The trends in environmental tracers are consistent with the GAB as a potential water source. For example, chloride and δ^2H in the Coonamble Embayment of the GAB vary between 10 and 90 mg L^{-1} and -46 and $-37‰$ VSMOW, respectively [*Radke et al.*, 2000], similar to that found in some of the deeper piezometers. While there is limited information for the Pilliga Sandstone, elsewhere along the margins of the GAB groundwater ^{4}He concentrations vary between 50 and 2600 $\times$ 10^{-8} cm^3 STP g^{-1} [*Bethke et al.*, 1999; *Mahara et al.*, 2009]. Another possibility for the elevated riparian ^{4}He concentrations could be that the upward diffusive flux from an underlying geological formation is greater than the downward advective flux [*Stute et al.*, 1992]. However, as ^{4}He concentrations in the alluvium near the surface appear as high as in the underlying GAB, a large upward diffusive ^{4}He flux from the GAB appears unlikely. The potential for leakage from underlying aquifers is not currently considered in the water balance for the Lower Namoi Alluvium and warrants further investigation.

5. Conclusion

Environmental tracers can be used to estimate infiltration rates at the riparian scale in environments like the Lower Namoi Alluvium, including at time scales (decades) often beyond what is possible with hydraulic gradient measurements when monitoring is recent or incomplete. However, because of a dynamic hydrological environment, tracer interpretation is complex and the derived infiltration rates have a high uncertainty at present. Longer-term monitoring in the river and in the piezometer network may improve both tracer and hydraulically derived infiltration rates by, for example, reducing the uncertainty associated with the tracer input function to the aquifer and averaging the hydraulic signals [*Stolp et al.*, 2010]. Longer-term records would also enable to interpret the tracer data using more realistic nonsteady state groundwater flow models when compared to the simple lumped parameter models used here.

References

Aeschbach-Hertig, W., F. Peeters, U. Beyerle, and R. Kipfer (1999), Interpretation of dissolved atmospheric noble gases in natural waters, *Water Resour. Res.*, 35, 2779–2792.

Aeschbach-Hertig, W., F. Peeters, U. Beyerle, and R. Kipfer (2000), Palaeotemperature reconstruction from noble gases in ground water taking into account equilibration with entrapped air, *Nature*, 405, 1040–1044.

Aggarwal, P. K., L. Araguas-Araguas, M. Gröning, B. Newman, T. Kurttas, W. Papesch, D. Rank, A. Suckow, and T. Vitvar (2010), Long-term tritium monitoring to study river basin dynamics: Case of the Danube River basin, *Geophys. Res. Abstr.*, 12. [Available at http://meetingorganizer.copernicus.org/EGU2010/EGU2010-11775.pdf.]

Bertin, C. B., and A. C. Bourg (1994), Radon-222 and chloride as natural tracers of the infiltration or river water into an alluvial aquifer in which there is significant river/groundwater mixing, *Environ. Sci. Technol.*, 28(5), 794–798.

Bethke, C. M., X. Zhao, and T. Torgersen (1999), Groundwater flow and the [4]He distribution in the Great Artesian Basin of Australia, *J. Geophys. Res.*, *104*, 12,999–13,011.

Beyerle, U., W. Aeschbach-Hertig, M. Hofer, D. M. Imboden, H. Baur, and R. Kipfer (1999), Infiltration of river water to a shallow aquifer investigated with ^{3}H/[3]He, noble gases and CFCs, *J. Hydrol.*, *220*, 169–185.

Brunner, P., P. G. Cook, and C. T. Simmons (2009), Hydrogeologic controls on disconnection between surface water and groundwater, *Water Resour. Res.*, *45*, W01422, doi:10.1029/2008WR006953.

Brunner, P., C. T. Simmons, P. G. Cook, and R. Therrien (2010), Modelling surface water-groundwater interaction with MODFLOW: Some considerations, *Ground Water*, *48*(2), 174–180.

Clark, I. D., and P. Fritz (1997), *Enviomental Isotopes in Hydrogeology*, 328 pp., A. F. Lewis, N. Y.

Constantz, J. (2008), Heat as a tracer to determine streambed water exchanges, *Water Resour. Res.*, *44*, W00D10, doi:10.1029/2008WR006996.

Cook, P. G., and J. K. Böhlke (2000), Determining timescales for groundwater flow and solute transport, in *Environmnetal Tracers in Subsurface Hydrology*, edited by P. G. Cook and A. L. Herczeg, pp. 1–30, Kluwer Acad., London, U. K.

Crosbie, R., D. Morrow, R. Cresswell, F. Leaney, S. Lamontagne, and M. Lefournour (2012), *New Insight to the Chemical and Isotopic Composition of Rainfall Across Australia*, CSIRO Water for a Healthy Country Flagship, Canberra, ACT, Australia. [Available at https://publications.csiro.au/rpr/download?pid=csiro:EP125581&dsid=DS4.]

CSIRO (2007), Water availability in the Namoi, A report to the Australian Government from the CSIRO Murray-Darling Basin Sustainable Yields Project, report, 154 pp., Canberra, ACT, Australia. [Available at http://www.clw.csiro.au/publications/waterforahealthycountry/mdbsy/pdf/Namoi-Report.pdf.]

Eastoe, C., W. R. Hutchison, B. J. Hibbs, J. Hawley, and J. F. Hogan (2010), Interaction of a river with an alluvial aquifer: Stable isotopes, salinity and water budgets, *J. Hydrol.*, *395*, 67–78.

Fallon, S. J., L. K. Fifield, and J. M. Chappell (2010), The next chapter in radiocarbon dating at the Australian National University: Status report on the single AMS, *Nucl. Instrum. Methods Phys. Res., Sect. B*, *268*, 898–901.

Freeze, R. A., and J. A. Cherry (1979), *Groundwater*, 604 pp., Prentice Hall, Englewood Cliffs, N. J.

Gardner, P., and D. K. Solomon (2009), An advanced passive diffusion sampler for the determination of dissolved gas concentrations, *Water Resour. Res.*, *45*, W06523, doi:10.1029/2008WR007394.

Herczeg, A. L. (2008), Background report on the Great Artesian Basin, report, 18 pp., CSIRO, Canberra, ACT, Australia. [Available at http://www.clw.csiro.au/publications/waterforahealthycountry/mdbsy/technical/S-GreatArtesianBasin.pdf.]

Hoehn, E., and H. R. von Gunten (1989), Radon in groundwater: A tool to assess infiltration from surface waters to aquifers, *Water Resour Res.*, *25*, 1795–1803.

Kalin, R. M. (2000), Radiocarbon dating of groundwater systems, in *Environmental Tracers in Subsurface Hydrology*, edited by P. G. Cook and A. L. Herczeg, pp. 111–142, Kluwer Acad., London, U. K.

Kirchner, J. W., X. H. Feng, and C. Neal (2000), Fractal stream chemistry and its implications for contaminant transport in catchments, *Nature*, *403*, 524–527.

Kulongoski, J. T., and J. A. Izbicki (2008), Simulation of fluid, heat transport to estimate desert stream infiltration, *Ground Water*, *46*, 462–474.

Labasque, T., L. Aquilina, V. Vergnaud, F. Barbecot, and Contributors from participating laboratories (2014), Inter-laboratory comparison of the analyses of sulphur hexafluroride (SF$_6$) and the three chlorofluorocarbons (CFC-11, −12 and −113) in groundwater and an air standard, *Appl. Geochem.*, *50*, 118–129, doi:10.1016/j.apgeochem.2014.03.009.

Lamontagne, S., A. R. Taylor, P. G. Cook, R. S. Crosbie, R. Brownbill, R. M. Williams, and P. Brunner (2014), Field assessment of surface water-groundwater connectivity in a semi-arid river basin (Murray-Darling, Australia), *Hydrol. Processes*, *28*, 1561–1572, doi:10.1002/hyp.9691.

Mahara, Y., et al. (2009), Groundwater dating by estimation of groundwater flow velocity and dissolved [4]He accumulation rate calibrated by [36]Cl in the Great Artesian Basin, Australia, *Earth Planet. Sci. Lett.*, *287*, 43–56.

Maiss, M., and C. A. M. Brenninkmeijer (1998), Atmospheric SF$_6$: Trends, sources and prospects, *Environ. Sci. Technol.*, *32*, 3077–3086.

Maiss, M. H., and I. Levin (1994), Global increase of SF$_6$ observed in the atmosphere, *Geophys. Res. Lett.*, *21*, 569–572.

Maloszewski, P., and A. Zuber (1982), Determining the turnover time of groundwater systems with the aid of environmental tracers. I. Models and their applicability. *J. Hydrol.*, *57*, 207–231.

McCallum, A. M., M. S. Andersen, B. M. S. Giambastiani, B. F. J. Kelly, and R. I. Acworth (2013), River-aquifer interactions in a semi-arid environment stressed by groundwater abstraction, *Hydrol. Processes*, *27*, 1072–1085.

McCallum, A. M., M. S. Andersen, and R. I. Acworth (2014), A new method for estimating recharge to unconfined aquifers using differential river gauging, *Ground Water*, *52*(2), 291–297, doi:10.1111/gwat.12046.

Morgenstern, U., and C. B. Taylor (2009), Ultra low-level tritium measurements using electrolytic enrichment and LSC, *Isotopes Environ. Health Stud.*, *45*, 96–117.

Morgenstern, U., M. K. Stewart, and R. Stenger (2010), Dating of streamwater using tritium in a post nuclear bomb pulse world: Continuous variation of mean transit time with streamflow, *Hydrol. Earth Syst. Sci.*, *14*, 2289–2301.

Parsons, S., R. Evans, and M. Hoban (2008), Surface-groundwater connectivity assessment. A report to the Australian Government from the CSIRO Murray-Darling Basin Sustainable Yields Project, report, 34 pp., CSIRO, Canberra, ACT, Australia. [Available at http://www.clw.csiro.au/publications/waterforahealthycountry/mdbsy/technical/R-SW-GW-Connectivity.pdf.]

Plummer, L. N., and E. Busenberg (2000), Chlorofluorocarbons, in *Environmental Tracers in Subsurface Hydrology*, edited by P. G. Cook and A. L. Herczeg, pp. 441–478, Kluwer Acad., London, U. K.

Poole, J. C., G. W. McNeill, S. R. Langman, and F. Dennis (1997), Analysis of noble gases in water using a quadrupole mass spectrometer in static mode, *Appl. Geochem.*, *12*, 707–714.

Radke, B. M., R. G. Ferguson, T. R. Cresswell, T. R. Ransley, and M. A. Habermehl (2000), *Hydrochemistry and Implied Hydrodynamics of the Cadna-Owie–Hooray Aquifer Great Artesian Basin, Australia*, 229 pp., Bur. of Rural Sci., Canberra.

Rassam, D., G. Walker, and B. Barnett (2008), Recommendations for modelling surface-groundwater interactions based on lessons learnt from the Murray-Darling Basin Sustainable Yields Project, report, 33 pp., CSIRO, Canberra, ACT, Australia. [Available at https://publications.csiro.au/rpr/download?pid=procite:e8f0ed31–693f-4def-9543-717bd3dfb07f&dsid=DS1.]

Rassam, D. W. (2011), A conceptual framework for incorporating surface-groundwater interactions into a river operation–planning model, *Environ. Modell. Software*, *26*, 1554–1567, doi:10.1016/j.envsoft.2011.07.019.

Rassam, D. W., L. Peeters, T. Pickett, I. Jolly, and L. Holz (2013), Accounting for surface–groundwater interactions and their uncertainty in river and groundwater models: A case study in the Namoi River, Australia, *Environ. Modell. Software*, *50*, 108–119, doi:10.1016/j.envsoft.2013.09.004.

Schmadel, N. M., B. T. Neilson, and D. K. Stevens (2010), Approaches to estimate uncertainty in longitudinal channel water balances, *J. Hydrol.*, *394*, 357–369.

Simpson, H. J., and A. L. Herczeg (1991), Stable isotopes as an indicator of evaporation in the River Murray, Australia, *Water Resour. Res.*, *27*, 1925–1935.

Smerdon, B. D., T. R. Ransley, B. M. Radke, and J. R. Kellet (2012), *Water Resource Assessment for the Great Artesian Basin*, 45 pp., CSIRO Water for a Healthy Country Flagship, Canberra, ACT, Australia. [Available at https://publications.csiro.au/rpr/download?pid=csiro:EP132686 &dsid=DS5.]

Solomon, D. K. (2000), ^{4}He in groundwater, in *Environmental Tracers in Subsurface Hydrology*, edited by P. G. Cook and A. L. Herczeg, pp. 425–440, Kluwer Acad., London, U. K.

Solomon, D. K., and P. G. Cook (2000), ^{3}H and ^{3}He, in *Environmental Tracers in Subsurface Hydrology*, edited by P. G. Cook and A. L. Herczeg, pp. 397–424, Kluwer Acad., London, U. K.

Solomon, D. K., A. Hunt, and R. J. Poreda (1996), Source of radiogenic helium-4 in shallow aquifers: Implications for dating young ground-water, *Water Resour. Res.*, *32*, 1805–1813.

Sophocleous, M., M. A. Townsend, L. D. Vogler, T. J. McClain, E. T. Marks, and G. R. Coble (1988), Experimental studies in stream aquifer interaction along the Arkansas River in Central Kansas—Field testing and analysis, *J. Hydrol.*, *98*, 249–273.

Stewart, M. K., U. Morgenstern, J. J. McDonnell, and L. Pfister (2012), The 'hidden streamflow' challenge in catchment hydrology, *Hydrol. Processes*, *26*, 2061–2066.

Stolp, B. J., D. K. Solomon, A. Suckow, T. Vitvar, D. Rank, P. K. Aggarwal, and L. F. Han (2010), Age-dating base flow at springs and gaining streams using helium-3 and tritium: Fischa-Dagnitz system, southern Vienna, Austria, *Water Resour. Res.*, *46*, W07503, doi:10.1029/2009WR008006.

Stute, M., and P. Schlosser (1993), Principles and applications of the Noble Gas Paleothermometer, in *Climate Change in Continental Isotopic Records*, edited by P. K. Swart et al., pp. 89–100, AGU, Washington, D. C.

Stute, M., C. Sonntag, J. Deak, and P. Schlosser (1992), Helium in deep circulating groundwater in the Great Hungarian Plain—Flow dynamics and crustal and mantle helium fluxes, *Geochim. Cosmochim. Acta*, *56*, 2051–2067.

Stute, M., M. Forster, H. Frischkorn, A. Serejo, J. F. Clark, P. Schlosser, W. S. Broecker, and G. Bonani (1995), Cooling of tropical Brazil (5°C) during the Last Glaxial Maximum, *Science*, *269*, 379–383.

Suckow, A. (2012), Lumpy—An interactive Lumped Parameter Modelling code based on MS Access and MS Excel, *Geophys. Res. Abstr.*, *14*. [Available at http://meetingorganizer.copernicus.org/EGU2012/EGU2012-2763.pdf.]

Tadros, C. V., C. E. Hughes, J. Crawford, S. E. Hollins, and R. Chisari (2014), Tritium in Australian precipitation: A 50 year record, *J. Hydrol.*, *513*, 262–273, doi:10.1016/j.hydrol.2014.03.031.

Taylor, A. R., S. Lamontagne, and R. S. Crosbie (2013), Measurements of riverbed hydraulic conductivity in a semi-arid lowland river system (Murray-Daling Basin, Australia), *Soil Res.*, *51*, 363–371, doi:10.1071/SR13090.

Vázquez-Suñé, E., B. Capino, E. Abarca, and J. Carrera (2007), Estimation of recharge from floods in disconnected stream-aquifer systems, *Ground Water*, *45*, 579–589.

Visser, A., E. Fourré, F. Barbecot, L. Aquilina, T. Labasque, V. Vergnaud, B. K. Esser, and Contributors from participating laboratories (2014), Intercomparison of tritium and noble gases analyses, ^{3}H/^{3}He ages and derived parameters excess air and recharge temperature, *Appl. Geochem.*, *50*, 130–141, doi:10.1016/j.apgeochem.2014.03.005.

Vogel, J. C. (1967), Investigation of groundwater flow with radiocarbon, in *Isotopes in Hydrology*, pp. 355–369, IAEA, Vienna.

Weissman, G. S., Y. Zhang, E. M. LaBolle, and G. E. Fogg (2002), Dispersion of groundwater age in an alluvial aquifer system, *Water Resour. Res.*, *38*(10), 1198, doi:10.1029/2001WR000907.